Towards Minimizing Feature Drift in Model Merging: Layer-wise Task Vector Fusion for Adaptive Knowledge Integration

Wenju Sun^{1,2}, Qingyong Li^{1,3,*}, Wen Wang^{1,2}, Yang Liu^{1,2}, Yangliao Geng^{1,2,*}Boyang Li⁴

¹Key Laboratory of Big Data & Artificial Intelligence in Transportation, Beijing, China

²School of Computer Science and Technology, Beijing Jiaotong University, Beijing, China

³Frontiers Science Center for Smart High-Speed Railway System,

Beijing Jiaotong University, Beijing, China

⁴College of Computing and Data Science, Nanyang Technological University, Singapore

{sunwenju, liqy, wangwen, yliucit, gengyla}@bjtu.edu.cn

boyang.li@ntu.edu.sg

Abstract

Multi-task model merging aims to consolidate knowledge from multiple fine-tuned task-specific experts into a unified model while minimizing performance degradation. Existing methods primarily approach this by minimizing differences between task-specific experts and the unified model, either from a parameter-level or a task-loss perspective. However, parameter-level methods exhibit a significant performance gap compared to the upper bound, while task-loss approaches entail costly secondary training procedures. In contrast, we observe that performance degradation closely correlates with feature drift, i.e., differences in feature representations of the same sample caused by model merging. Motivated by this observation, we propose Layer-wise Optimal Task Vector Merging (LOT Merging), a technique that explicitly minimizes feature drift between task-specific experts and the unified model in a layer-by-layer manner. LOT Merging can be formulated as a convex quadratic optimization problem, enabling us to analytically derive closed-form solutions for the parameters of linear and normalization layers. Consequently, LOT Merging achieves efficient model consolidation through basic matrix operations. Extensive experiments across vision and vision-language benchmarks demonstrate that LOT Merging significantly outperforms baseline methods, achieving improvements of up to 4.4% (ViT-B/32) over state-of-the-art approaches. The source code is available at https://github.com/SunWenJu123/model-merging.

1 Introduction

Pretrained foundational models [24, 4] encapsulate rich, transferable knowledge, which has facilitated their widespread use for fine-tuning on downstream tasks, yielding superior performance. However, the predominant use of the pretraining-finetuning paradigm has resulted in a proliferation of fine-tuned models, substantially increasing storage and maintenance costs for deployment. This challenge has driven the development of model merging, an effective strategy that consolidates the knowledge from multiple fine-tuned models into a single model, thereby eliminating the need for costly retraining.

Existing model merging methods typically focus on minimizing parameter differences between task-specific models and the merged model, such as arithmetic averaging of model parameters [12, 20] or generating masks based on heuristic factors [38, 5, 34]. These approaches aim to identify important

^{*}Correspondence to: Yangli-ao Geng <gengyla@bjtu.edu.cn> Qingyong Li liqy@bjtu.edu.cn>

parameters across different task models, attempting to preserve these key parameters during the merging process through weighting or masking strategies. While these methods are simple and efficient, their performance still lags behind the upper bound. Other approaches incorporate loss functions to train merging weights [41] or use adapter modules [40] during the merging phase. These techniques achieve impressive performance but are computationally expensive due to the need for secondary training.

In contrast to the aforementioned methods, our study investigates the performance degradation of merged models from the perspective of feature drift, i.e., differences in feature representations of the same sample caused by model merging. As illustrated in Figure 1(a), we observe a strong correlation between feature drift (measured by cosine distance) and the performance degradation associated with merging. Furthermore, Figure 1(b) demonstrates that feature drift becomes more pronounced as network depth increases, as small perturbations in the initial layers are progressively amplified through the layers of the network.

These findings motivate our proposal of Layer-wise Optimal Task vector Merging (LOT Merging), a method that explicitly minimizes feature drift across layers. Specifically, LOT Merging uses squared error to measure the feature difference be-

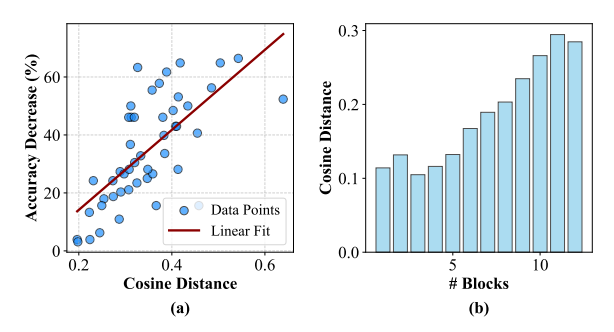


Figure 1: An illustration of feature drift (measured as the cosine distance between features extracted by task-specific expert models and the merged model) is presented using Task Arithmetic [12] on eight vision tasks. (a) The feature drift in the last layer shows a linear correlation with the accuracy decrease, with data points collected for each task under varying merging coefficients. (b) Feature drift becomes more pronounced as the network depth increases.

tween the merged model and task-specific models, which can be formulated as a convex quadratic optimization problem. Solving this problem analytically yields closed-form solutions for parameters in both linear and normalization layers, enabling efficient model consolidation via basic matrix operations. Additionally, we provide an intuitive explanation of LOT Merging through theoretical analysis in two extreme cases, illustrating its ability to adaptively adjust the merging strategy based on task dependencies. In summary, this paper makes the following contributions:

- We formulate the model merging task as a convex quadratic optimization problem by minimizing layer-wise feature drift, which enjoys a closed-form solution and such inspire an efficient model consolidation method referred to as LOT Merging.
- We provide a theoretical analysis of LOT Merging, revealing its resilient merging capabilities that effectively account for correlations among different task feature spaces.
- We conduct extensive experiments on a variety of visual and vision-language benchmarks, showing LOT Merging's superiority over state-of-the-art methods while maintaining robustness with limited exemplars.

2 Related Work

Model merging aims to integrate the knowledge of multiple fine-tuned models into a single model. Early work primarily focused on weighted averaging strategies, such as employing the Fisher information matrix [20], or minimizing the feature distance between the merged model and individual models [13]. Recent research on multi-task model merging is typically built upon "task vectors" [12], defined as the parameter differences between the pre-trained model and each fine-tuned counterpart. Task Arithmetic [12] demonstrates that simple operations on task vectors—such as addition—can be used to edit or merge knowledge effectively. Subsequent methods like Ties-Merging [38] and PCBMerging [5] improve upon this idea by pruning low-magnitude components from task vectors. Extensions to parameter-efficient fine-tuning settings include PEFT [42] and MoLE [35], which adapt Task Arithmetic to LoRA-based modules [10]. Additionally, some model merging methods rely on test-time training techniques. For instance, AdaMerging [41] learns a set of layer-wise merging coefficients via gradient descent; Surgery [40] introduces an auxiliary adapter module to

align intermediate representations; WEMoE [32] and Twin Merging [18] adopt mixture-of-experts frameworks and train a router to select among experts; and Localize-and-Stitch [7] constructs a binary mask that determines which parameters to merge. Since the training requires constructing computation graphs to achieve gradient descent, the memory and computation overhead of such methods tend to be expensive when applied to large-scale foundation models.

This paper introduces a layer-wise merging strategy for task vectors in parameter space, aiming to mitigate feature drift during model merging. By analyzing three parameter types in transformer architectures—linear weights, scaling factors, and bias terms—we derive closed-form solutions that enable efficient and principled integration. While our solution for linear weights parallels RegMean [13], our formulation operates on task vectors rather than original parameters, marking a fundamental distinction (see Section 5.2). Moreover, our method extends beyond RegMean by addressing additional parameter types and offering a deeper understanding of the mechanisms behind LOT merging. Compared to RegMean, our approach yields improvements of 10.9% (ViT-B/32) and 6.8% (ViT-L/14), and remains effective in dataless scenarios. Additionally, our method shares the goal of mitigating feature drift with Surgery [40] and CAT Merging [29], but differs in approach. Surgery introduces a test-time alignment module, whereas our method is entirely training-free. Unlike CAT Merging, which constructs bases or masks to trim task vectors, we derive a direct closed-form solution for optimal merging, resulting in further performance improvements.

3 Preliminary

3.1 Model Merging

Problem setup. Consider a pre-trained model characterized as an L-layer neural network $W_{\text{pre}} = \{W_{\text{pre}}^l\}_{l=1}^L$, where W_{pre}^l represents the parameters of the l-th layer. Starting from W_{pre} , we fine-tune it independently on K down-stream tasks, resulting in task-specific expert models $\{W_1,\ldots,W_K\}$. The objective is to merge these fine-tuned experts into a single unified model W_{mtl} without the need for redundant retraining.

Task Vector. To facilitate model merging, Task Arithmetic [12] introduces the concept of *task vector*, defined as the parameter difference between the fine-tuned expert W_k and W_{pre} :

$$T_k = W_k - W_{\text{pre}},\tag{1}$$

where the arithmetic operations over parameter sets are applied layer-by-layer, i.e., $W_k - W_{\rm pre} = \{W_k^l - W_{\rm pre}^l\}_{l=1}^L$. Task Arithmetic has demonstrated that performing simple arithmetic operations over task vectors can effectively integrate knowledge into the pre-trained model:

$$W_{\text{mtl}}^{\text{ta}} = W_{\text{pre}} + \lambda \sum_{k=1}^{K} T_k, \tag{2}$$

where the addition is performed layer-wise and λ is a manually defined scaling factor.

Resource limitations. In practice, it is often infeasible to access the full downstream training sets, yet most existing merging techniques still depend on some form of data-driven calibration. For instance, Fisher Merging [20], TATR [30], and CAT Merging [29] require a subset of labeled examples to estimate parameter importance, while approaches such as Task Arithmetic and Ties-Merging rely on a validation set to select hyperparameters. In addition, test-time adaptation methods require access to unlabeled examples at inference time to adjust the merging weights or train additional modules. These methods typically require iterative backpropagation, making them impractical under constrained GPU resources to merge large-scale models. In contrast, our method is entirely training-free, incurs only a handful of forward passes with a small sample set.

3.2 Negative Transfer

One major challenge in model merging is the negative transfer [38, 30], which occurs when the knowledge acquired by individual models conflicts or interferes with one another. Mathematically, negative transfer can be quantified by the degradation in performance across tasks resulting from the merging process. Let $\mathcal{L}_k(\cdot)$ denote the loss for task k, the negative transfer introduced by the merging

task vector T (where for task arithmetic, $T = \lambda \sum_{k=1}^{K} T_k$) can then be defined as follows:

$$\Delta \mathcal{L}_{k} = \mathcal{L}_{k} \left(W_{\text{pre}} + T \right) - \mathcal{L}_{k} \left(W_{k} \right). \tag{3}$$

However, analyzing this degradation is often challenging due to the hierarchical structure inherent in deep neural networks. Instead, this work examines layer-wise negative transfer in the form of feature drift. Let $f_k^l(W_k)$ be the representation produced by the layer l of the model W on the samples of task k. Then, the layer-specific feature drift caused is formulated as:

$$\Delta f_k^l = f_k^l \left(W_{\text{pre}} + T^l \right) - f_k^l \left(W_k \right). \tag{4}$$

where $W_{\text{pre}}+T^l$ denotes the model parameters with only the l-th layer merged, i.e., $W_{\text{pre}}+T^l=\{W_{\text{pre}}^1,\ldots,W_{\text{pre}}^{l-1},W_{\text{pre}}^l+T^l,W_{\text{pre}}^{l+1}\ldots,W_{\text{pre}}^L\}.$

Sun et al. [29] have derived that the feature drift of every layer contributes to the overall negative transfer, yielding the following upper bound of knowledge conflict:

$$|\Delta \mathcal{L}_k| \le \beta \sum_{l=1}^L \left(\prod_{m=l+1}^L \gamma_m \right) \|\Delta f_k^l\|. \tag{5}$$

where \mathcal{L}_k is assumed β -Lipschitz continuous with respect to the network's final output, and the function implemented by each layer l is γ_l -Lipschitz continuous with respect to its input (i.e., the output of layer l-1) within the merging region. For a detailed proof, please refer to Section B.

4 Method

Motivated by Eq. (5), our approach aims to mitigate knowledges conflicts by minimizing the feature drift $\|\Delta f_k^l\|$ for each layer l. Specifically, we pursue an optimal shared task vector T^{l^*} by solving the following optimization problem:

$$T^{l^{\star}} = \arg\min_{T^{l}} \sum_{k=1}^{K} \|\Delta f_{k}^{l}\|^{2} = \arg\min_{T^{l}} \sum_{k=1}^{K} \|f_{k}^{l}(W_{\text{pre}} + T^{l}) - f_{k}^{l}(W_{k})\|^{2}.$$
 (6)

The computation of T^{l^*} depends on the specific form of $f^l(\cdot)$. In transformer-based architectures, all such operations can be categorized into the following three types:

- Matrix multiplication, corresponding to the weight parameters of linear layers;
- Element-wise (Hadamard) products, corresponding to the scaling factors in normalization layers:
- **Element-wise addition**, corresponding to the bias parameters of linear layers and the shifting factors in normalization layers.

In our analysis, we treat each minimal computational unit independently. For example, the weight and bias components of a linear layer are considered as separate layers to facilitate analysis. Similarly, in complex modules such as attention blocks, the computations of queries, keys, and values (QKV) are disentangled and analyzed as independent layers. It is also worth noting that the convolutional operation can be equivalently expressed as matrix multiplication [31]. Therefore, we do not treat it as a separate category in our analysis. In the following, we discuss these three types of operations and present the closed-form solution T^{l^*} for each case.

4.1 Solution for Matrix Multiplication

Suppose $W^l \in \mathbb{R}^{d_l \times d_{l+1}}$ corresponds to the weight of a linear layer, which transforms features through matrix multiplication. Specifically, for task k, given the input feature matrix $X_k^l \in \mathbb{R}^{n \times d_l}$ extracted by the first l-1 layers, the transformed feature representation is expressed as:

$$f_k^l(W) = X_k^l W^l. (7)$$

Substituting Eq. (7) into Eq. (6) yields the following objective:

$$T^{l^{*}} = \arg\min_{T^{l}} \sum_{k=1}^{K} \|X_{k}^{l}(W_{\text{pre}}^{l} + T^{l}) - X_{k}^{l}(W_{k}^{l})\|_{F}^{2}$$

$$= \arg\min_{T^{l}} \sum_{k=1}^{K} \|X_{k}^{l}(T^{l} - T_{k}^{l})\|_{F}^{2} = \arg\min_{T^{l}} \sum_{k=1}^{K} \operatorname{trace}((T^{l} - T_{k}^{l})^{\top} X_{k}^{l^{\top}} X_{k}^{l} (T^{l} - T_{k}^{l})).$$
(8)

This defines a convex quadratic optimization problem. Consequently, the optimal solution T^{l^*} can be derived in closed form as follows:

$$T^{l^{\star}} = \left(\sum_{k} X_{k}^{l} {}^{\top} X_{k}^{l}\right)^{\dagger} \sum_{k} X_{k}^{l} {}^{\top} X_{k}^{l} T_{k}^{l}, \tag{9}$$

where † denotes the Moore-Penrose inverse [9].

4.2 Solution for Element-Wise (Hadamard) Multiplication

Next, consider the case where $W^l \in \mathbb{R}^{d_l}$ represents the scaling factors in a normalization layer, i.e.,

$$f_k^l(W) = X_k^l \circ W^l = \left[\dots, x_k^l \circ W^l, \dots\right]^\top, \tag{10}$$

where \circ denotes the element-wise product and x_k^l represents a sample feature in X_k^l . Under this setting, the objective can be formulated as

$$T^{l} \stackrel{\star}{=} \underset{T^{l}}{\arg\min} \sum_{k=1}^{K} \sum_{x_{k}^{l}} \|x_{k}^{l} \circ (W_{\text{pre}}^{l} + T^{l}) - x_{k}^{l} \circ (W_{k}^{l})\|^{2} = \underset{T^{l}}{\arg\min} \sum_{k=1}^{K} \sum_{x_{k}^{l}} \sum_{d=1}^{d_{l}} x_{k}^{l} [d]^{2} (T^{l}[d] - T_{k}^{l}[d])^{2},$$

$$(11)$$

where x[d] represents the d-th dimension of x. By setting the derivative of the objective with respect to $T^{l}[d]$ to zero, we obtain the closed-form solution:

$$T^{l^{\star}}[d] = \frac{\sum_{k=1}^{K} \sum_{x_k^l} x_k^l[d]^2 T_k^l[d]}{\sum_{k=1}^{K} \sum_{x_k^l} x_k^l[d]^2}.$$
 (12)

4.3 Solution for Element-Wise Addition

Suppose $W^l \in \mathbb{R}^{d_l}$ represents the bias coefficients, which are added element-wise to X_k^l :

$$f_k^l(W) = X_k^l + W^l = \left[\dots, x_k^l + W^l, \dots\right]^{\top}.$$
 (13)

Thus, the optimal solution can be derived as follows:

$$T^{l^{\star}} = \underset{T^{l}}{\arg\min} \sum_{k=1}^{K} \sum_{x_{k}^{l}} \|x_{k}^{l} + (W_{\text{pre}}^{l} + T^{l}) - (x_{k}^{l} + W_{k}^{l})\|^{2} = \underset{T^{l}}{\arg\min} \sum_{k=1}^{K} \|T^{l} - T_{k}^{l}\|^{2} = \frac{1}{K} \sum_{k=1}^{K} T_{k}^{l}. \tag{14}$$

Now, we have derived the optimal vectors for all three types of operation. As summarized in Algorithm 1, we first perform a forward pass over a small exemplar set (16–64 samples per task) to extract each layer's input features for every expert. After obtaining T^* , we integrate it into the pre-trained parameters using a predefined weight λ :

$$W_{\rm mtl}^{\rm lot} = W_{\rm pre} + \lambda T^{\star}. \tag{15}$$

Empirically, setting $\lambda=1$ already yields competitive performance. However, further tuning of λ on a validation set, similar to the approach in Task Arithmetic, can lead to additional improvements (see Section 6.3 for a detailed sensitivity analysis).

5 Discussion

5.1 Exploring the Mechanism of LOT Merging

We present a theoretical analysis of the LOT Merging mechanism, focusing on the behavior of merging matrix-multiplication parameters. Specifically, we apply singular value decomposition (SVD) to the input feature matrices at a given layer l, where the representation for task k is given by $X_k^l = U_k^l \Sigma_k^l V_k^{l^\top}$. To gain insight into the behavior of LOT Merging, we analyze two extreme cases: (1) the *ideal case* in which task-specific features are mutually orthogonal, and (2) the *worst case* where task-specific features are fully collinear.

Ideal case. Assume that for any pair of distinct tasks $k \neq j$, their right singular vectors satisfy the orthogonality condition $V_k^{l^\top}V_j^l=0$. Under this condition, the optimal solution in Eq. (9) simplifies to a summation of the task vectors:

$$T_{\text{ideal}}^{l*} = \left(\sum_{k} V_{k}^{l} \Sigma_{k}^{l}^{2} V_{k}^{l}^{\top}\right)^{\dagger} \sum_{k} V_{k}^{l} \Sigma_{k}^{l}^{2} V_{k}^{l}^{\top} T_{k}^{l} = \sum_{k} \left(V_{k}^{l} \Sigma_{k}^{l}^{2} V_{k}^{l}^{\top}\right)^{\dagger} \sum_{k} V_{k}^{l} \Sigma_{k}^{l}^{2} V_{k}^{l}^{\top} T_{k}^{l} = \sum_{k} V_{k}^{l} V_{k}^{l}^{\top} T_{k}^{l}.$$

$$(16)$$

Here, the term $V_k^l V_k^{l^{\top}} T_k^l$ corresponds to a projection of T_k^l onto the subspace spanned by the singular vectors V_k^l . This projection retains only the components of T_k^l aligned with the corresponding feature space X_k^l , effectively filtering out irrelevant directions [31]. As a result, LOT Merging introduces no layer-wise feature drift:

$$\sum_{k=1}^{K} \|X_{k}^{l} (T_{ideal}^{l^{\star}} - T_{k}^{l})\|_{F}^{2} = \sum_{k=1}^{K} \|U_{k}^{l} \Sigma_{k}^{l} V_{k}^{l^{\top}} (\sum_{j} V_{j}^{l} V_{j}^{l^{\top}} T_{j}^{l} - T_{k}^{l})\|_{F}^{2}$$

$$= \sum_{k=1}^{K} \|U_{k}^{l} \Sigma_{k}^{l} V_{k}^{l^{\top}} V_{k}^{l} V_{k}^{l^{\top}} T_{k}^{l} - U_{k}^{l} \Sigma_{k}^{l} V_{k}^{l^{\top}} T_{k}^{l}\|_{F}^{2} = 0. \tag{17}$$

Worst case. Now we assume the opposite extreme condition that all task features share a common group of singular vectors, i.e., $V_k^l = V^l, \forall k$. Under this condition, the optimal solution in Eq. (9) becomes a weighted average within the shared subspace spanned by V^l :

$$T_{\text{worst}}^{l^{\star}} = \left(\sum_{k} V^{l} \Sigma_{k}^{l^{2}} V^{l^{\top}}\right)^{\dagger} \sum_{k} V^{l} \Sigma_{k}^{l^{2}} V^{l^{\top}} T_{k}^{l}$$

$$= V^{l} \left(\sum_{k} \Sigma_{k}^{l^{2}}\right)^{\dagger} V^{l^{\top}} \sum_{k} V^{l} \Sigma_{k}^{l^{2}} V^{l^{\top}} T_{k}^{l} = \sum_{k} \left(V^{l} \underbrace{\left(\sum_{k} \Sigma_{k}^{l^{2}}\right)^{\dagger} \Sigma_{k}^{l^{2}} V^{l^{\top}} T_{k}^{l}}_{Normalized Weight}\right). \tag{18}$$

While feature drift is unavoidable in this setting due to collinearity, the formulation ensures that the deviation is minimized through weighted averaging.

These two extreme cases highlight the adaptability of LOT Merging. In realistic settings where task representations are partially aligned, LOT Merging balances task specificity with shared structure, projecting task-specific transformations into relevant subspaces while aggregating shared patterns. This flexibility allows it to perform robustly across a range of multi-task learning scenarios.

5.2 Task Vector Merging vs. Parameter Merging

In this work, we aim to derive an optimal task vector for merging. A natural question arises: why not directly solve for the optimal merging parameters as done in [13]? To illustrate this, consider the direct merging of linear weights via the following objective:

Table 1: Multi-task performance when merging ViT-B/32 models on eight vision tasks. The best
performance among training-free methods is highlighted with bold . The "#best" column represents
the number of datasets where the training-free method performs the best.

Method	SUN397	Cars	RESISC45	EuroSAT	SVHN	GTSRB	MNIST	DTD	Avg Acc	#best		
			Basic bas	seline metho	ds .							
Pre-trained	62.3	59.7	60.7	45.5	31.4	32.6	48.5	43.8	48.0	-		
Individual	75.3	77.7	96.1	99.7	97.5	98.7	99.7	79.4	90.5	-		
Traditional MTL	73.9	74.4	93.9	98.2	95.8	98.9	99.5	77.9	88.9	-		
Training-free methods												
Weight Averaging	65.3	63.4	71.4	71.7	64.2	52.8	87.5	50.1	65.8	0		
Fisher Merging	68.6	69.2	70.7	66.4	72.9	51.1	87.9	59.9	68.3	2		
RegMean	65.3	63.5	75.6	78.6	78.1	67.4	93.7	52.0	71.8	0		
Task Arithmetic	55.2	54.9	66.7	78.9	80.2	69.7	97.3	50.4	69.1	0		
Ties-Merging	59.8	58.6	70.7	79.7	86.2	72.1	98.3	54.2	72.4	0		
TATR	62.7	59.3	72.3	82.3	80.5	72.6	97.0	55.4	72.8	0		
Ties-Merging & TATR	66.3	65.9	75.9	79.4	79.9	68.1	96.2	54.8	73.3	0		
Consensus Merging	65.7	63.6	76.5	77.2	81.7	70.3	97.0	57.1	73.6	0		
AWD Merging	63.5	61.9	72.6	84.9	85.1	79.1	98.1	56.7	75.2	0		
PCB Merging	63.8	62.0	77.1	80.6	87.5	78.5	98.7	58.4	75.8	1		
CAT Merging	68.1	65.4	80.5	89.5	85.5	78.5	98.6	60.7	78.3	0		
LOT Merging (ours)	67.7	67.5	85.7	94.9	93.4	89.8	98.7	63.6	82.7	6		

$$W^{l^{\star}} = \arg\min_{W^{l}} \sum_{k=1}^{K} \|X_{k}^{l} W^{l} - X_{k}^{l} W_{k}^{l}\|_{F}^{2} = \left(\sum_{k} X_{k}^{l} X_{k}^{l}\right)^{\dagger} \sum_{k} X_{k}^{l} X_{k}^{l} W_{k}^{l}.$$
(19)

While Eq. (19) provides a straightforward solution, it implicitly modifies the knowledge contained in the pre-trained weights. To make this explicit, we establish a connection with our proposed T^{l^*} :

$$W^{l^{\star}} = \underbrace{\left(\sum_{k} X_{k}^{l}^{\top} X_{k}^{l}\right)^{\dagger} \sum_{k} X_{k}^{l}^{\top} X_{k}^{l} W_{\text{pre}}^{l}}_{\text{Modifying Pre-trained Knowledge}} + \underbrace{\left(\sum_{k} X_{k}^{l}^{\top} X_{k}^{l}\right)^{\dagger} \sum_{k} X_{k}^{l}^{\top} X_{k}^{l} T_{k}^{l}}_{\text{C20}}.$$
(20)

This decomposition highlights a critical issue: when X_k^l is rank-deficient—which often occurs in practice due to limited exemplar data—the projection term tends to discard useful pre-trained knowledge. The resulting distortion can lead to *catastrophic forgetting* [6] of previously learned representations. To quantify this effect, we compare the accuracy of merged models using W^{l^*} against individual expert models under varying exemplar budgets. As shown in Figure 2, performance degrades significantly as the number of exemplars decreases, where the majority of this degradation stems from the alteration of the pre-trained weights.

Consequently, methods based on Eq. (19), such as [13], typically require large exemplar sets (e.g., 1600 samples per task) to maintain competitive performance [7]. In contrast, our method achieves superior accuracy with as few as 16 to 64 exemplars per task. This substantial reduction in data requirement highlights the effectiveness of our merging strategy in preserving pre-trained knowledge while flexibly adapting to new tasks.

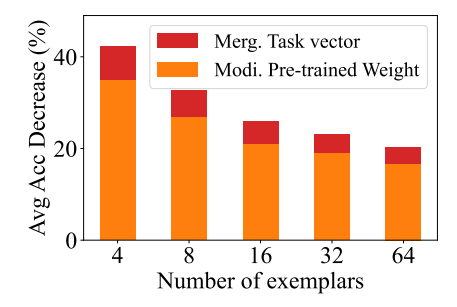


Figure 2: Performance (Avg ACC %) degradation of direct parameter merging compared to Individual under different numbers of exemplars when merging ViT-L/14 models. The error is decomposed into the impact of merging task vectors (red) and modifying pre-trained weights (orange).

Table 2: Multi-task performance when merging ViT-L/14 models on eight vision tasks.

Method	SUN397	Cars	RESISC45	EuroSAT	SVHN	GTSRB	MNIST	DTD	Avg Acc	#best		
			Basic bas	seline method	ds							
Pre-trained	66.8	77.7	71.0	59.9	58.4	50.5	76.3	55.3	64.5	-		
Individual	82.3	92.4	97.4	100.0	98.1	99.2	99.7	84.1	94.2	-		
Traditional MTL	80.8	90.6	96.3	96.3	97.6	99.1	99.6	84.4	93.5	-		
Training-free methods												
Weight Averaging	72.1	81.6	82.6	91.9	78.2	70.7	97.1	62.8	79.6	0		
Fisher Merging	69.2	88.6	87.5	93.5	80.6	74.8	93.3	70.0	82.2	1		
RegMean	73.3	81.8	86.1	97.0	88.0	84.2	98.5	60.8	83.7	0		
Task Arithmetic	73.9	82.1	86.6	94.1	87.9	86.7	98.9	65.6	84.5	0		
Ties-Merging	76.5	85.0	89.3	95.7	90.3	83.3	99.0	68.8	86.0	0		
TATR	74.6	83.7	87.6	93.7	88.6	88.1	99.0	66.8	85.3	0		
Ties-Merging & TATR	76.3	85.3	88.8	94.4	90.8	88.7	99.2	68.8	86.5	0		
Consensus Merging	75.0	84.3	89.4	95.6	88.3	82.4	98.9	68.0	85.2	0		
AWD Merging	76.2	85.4	88.7	96.1	92.4	92.3	99.3	69.4	87.5	0		
PCB Merging	76.2	86.0	89.6	95.9	89.9	92.3	99.2	71.4	87.6	0		
CAT Merging	78.7	88.5	91.1	96.3	91.3	95.7	99.4	75.7	89.6	2		
LOT Merging (ours)	76.7	88.6	91.7	98.7	97.1	95.7	99.5	76.4	90.5	7		

Table 3: Multi-task performance when merging BLIP models on six vision-language tasks.

Method	COCO Caption	Flickr30k Caption	Textcaps	OKVQA	TextVQA	ScienceQA	#best
Metric	CIDEr	CIDEr	CIDEr	Accuracy	Accuracy	Accuracy	
Pre-trained ·	0.07	0.03	0.05	42.80	21.08	40.50	-
Individual	1.17	0.65	0.65	50.84	29.79	76.89	-
Task Arithmetic	0.86	0.50	0.39	17.71	0.49	40.10	0
Ties-Merging	0.53	0.27	0.22	27.95	0.57	40.35	0
TATR	0.46	0.31	0.21	28.30	14.74	42.98	0
PCB Merging	0.71	0.52	0.30	36.04	1.88	43.01	0
CAT Merging	0.91	0.53	0.36	44.07	19.69	46.36	2
LOT Merging (ours)	0.91	0.54	0.44	38.35	20.82	48.24	5

6 Experiments

6.1 Settings

Benchmarks. Our experiments cover vision and vision-language tasks. For the vision tasks, we follow [12] and utilize eight image classification datasets: SUN397 [36], Cars [14], RESISC45 [2], EuroSAT [8], SVHN [22], GTSRB [28], MNIST [15], and DTD [3]. For the vision-language tasks, we focus on three captioning datasets (COCO Caption [1], Flickr30k Caption [23], Textcaps [26]) and three Visual Question Answering (VQA) datasets (OKVQA [19], TextVQA [27], and ScienceQA [17]).

Baselines. We select several training-free model merging methods as the primary comparison baselines, including weight averaging, Fisher Merging [20], RegMean [13], Task Arithmetic [12], Ties-Merging [38], TATR [30], Ties-Merging & TATR [30], Consensus Merging [34], AWD Merging [37], PCB Merging [5], and CAT Merging [29]. We also present three baseline methods for reference: Pre-trained model performance, Individual fine-tuned model performance, and Traditional Multi-Task Learning (MTL) performance.

Metrics. For both classification and VQA tasks, we employ accuracy as the evaluation metric. For captioning tasks, we select CIDEr as the evaluation criterion. To minimize potential performance fluctuations arising from the selection of different exemplar sets, we rerun LOT Merging with three randomly selected exemplar sets and report the average performance.

Implementation details. For vision tasks, following [12], we utilize the vision encoder of CLIP [24] as the pre-trained model, including both ViT-B/32 and ViT-L/14 versions. The task vectors are obtained from the official repository of [12]. When merging vision-language tasks, task vectors are generated by fine-tuning the VQA version of BLIP [25] for 6000 steps per task. The BLIP architecture consists of an image encoder, a text encoder, and a text decoder, with all model weights fine-tuned during training. Further details of the experiments can be found in our supplementary appendix and code. All exemplar sets are randomly sampled from the training set and are kept strictly separate from the test set used for evaluation.

6.2 Comparison Results

Merging ViT-B/32 models on vision tasks. We first compare multi-task performance when merging ViT-B/32 models on eight vision tasks (Table 1). Among the training-free methods, Fisher Merging achieves the highest accuracy on SUN397 and Cars, while our approach performs the best on all the remaining six tasks. Notably, our approach achieves the highest average accuracy of 82.7%, suppressing the second-best training-free methods with 4.4%.

Merging ViT-L/14 models on vision tasks. Next, we evaluate the multi-task performance when merging ViT-L/14 models on eight vision tasks (Table 2). Our method also achieves the highest average accuracy of 90.5%, higher than the second-best performance by 0.9%. Furthermore, our method performs best in seven tasks, confirming its robustness.

Merging vision-language tasks. Finally, we compare multi-task performance across six vision-language tasks when merging BLIP models (Table 3). Our method leads the performance with the highest CIDEr scores on COCO Caption, Flickr30k Caption, and Textcaps, as well as the highest accuracy on TextVQA and ScienceQA. In total, our method delivers the best performance in five tasks, showcasing its adaptability in vision-language tasks.

6.3 Sensitivity Analysis

Sensitivity analysis of exemplar number. The number of exemplars impacts LOT Merging by influencing the accuracy of $X^{l^{\top}}X^{l}$. As shown in Figure 3 (a), the performance of LOT Merging steadily improves as the number of exemplars increases. Notably, when the number of samples reaches only 16 per task, performance stabilizes with respect to the exemplar number. This demonstrates the robustness of LOT Merging in data-less scenarios (e.g., 16 samples per task). Based on our experiments, we empirically recommend using 64 samples per task.

Sensitivity analysis of λ (scaling factor in Eq. (15)). The scaling factor λ controls the contribution of task vectors to the merged model. As illustrated in Figure 3 (b), performance remains relatively stable for λ values in the range of 1.0 to 1.5. For larger

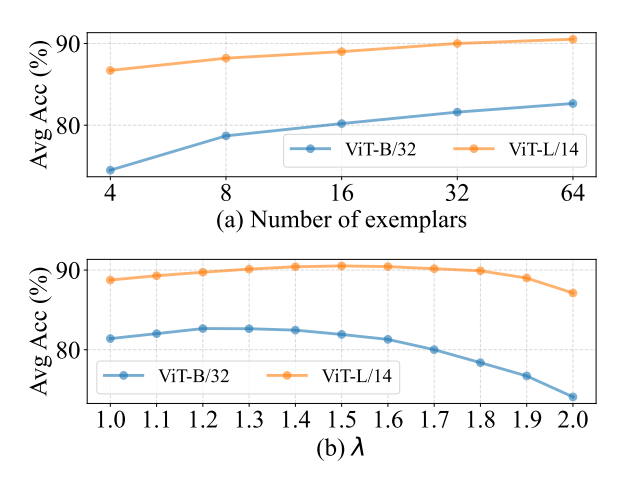


Figure 3: Average accuracy (%) on eight vision tasks with various numbers of exemplars (a) and λ (scaling factor in Eq. (15)).

values of λ , performance gradually decreases. Based on our empirical analysis, we set λ to 1.2 for merging ViT-B/32 and 1.5 for merging ViT-L/14.

7 Conlusion

In this paper, we propose Layer-wise Optimal Task Vector Merging (LOT Merging), a novel approach to mitigate the problem of feature drift in model merging. By adaptively merging task-specific knowledge at the layer level, LOT Merging reorganizes the merging process as an optimization task that minimizes the discrepancy between the representations of individual models before and after merging. This adaptive strategy ensures that task-specific information is retained while minimizing interference across tasks. LOT Merging requires no retraining and is suitable for scenarios with limited samples, making it highly efficient and applicable in resource-constrained environments. Our experiments on both vision and vision-language benchmarks demonstrate that LOT Merging significantly outperforms baseline methods, achieving up to 4.4% improvement on vision tasks and showing strong performance across various vision-language tasks.

While LOT Merging achieves strong empirical results with minimal data, it still requires access to a small exemplar set, which may not be feasible in strictly data-free scenarios. In addition,

although the method supports mainstream transformer architectures, extending it to models with more complex operations (e.g., layers involving exponential functions) may require additional adaptation. Future work could explore how feature drift interacts across layers to better disentangle conflicting knowledge and broaden the applicability of the approach.

Acknowledgments

This work was supported, in part, by the Fundamental Research Funds for the Central Universities under Grants 2025JBRC004, 2023JBZY037, and 2022JBQY007, by the Beijing Natural Science Foundation under Grant L231019, by the Hebei Natural Science Foundation under Grant F2025106045, by the National Natural Science Foundation of China under Grants 62276019, 62306028, 62501043, and U22B2004, by the Shenzhen Science and Technology Program Project under Grant KJZD20240903102742055, by the RIE2025 Industry Alignment Fund – Industry Collaboration Projects (IAF-ICP) (Award I2301E0026), administered by A*STAR, by Alibaba Group and NTU Singapore through Alibaba-NTU Global e-Sustainability CorpLab (ANGEL), and by the Nanyang Associate Professorship and National Research Foundation Fellowship (NRFF13-2021-0006), Singapore.

References

- [1] Xinlei Chen, Hao Fang, Tsung-Yi Lin, Ramakrishna Vedantam, Saurabh Gupta, Piotr Dollár, and C Lawrence Zitnick. Microsoft coco captions: Data collection and evaluation server. *arXiv* preprint *arXiv*:1504.00325, 2015.
- [2] Gong Cheng, Junwei Han, and Xiaoqiang Lu. Remote sensing image scene classification: Benchmark and state of the art. *Proceedings of the IEEE*, 105(10):1865–1883, 2017.
- [3] Mircea Cimpoi, Subhransu Maji, Iasonas Kokkinos, Sammy Mohamed, and Andrea Vedaldi. Describing textures in the wild. In *IEEE Conference on Computer Vision and Pattern Recognition*, June 2014.
- [4] Alexey Dosovitskiy, Lucas Beyer, Alexander Kolesnikov, Dirk Weissenborn, Xiaohua Zhai, Thomas Unterthiner, Mostafa Dehghani, Matthias Minderer, Georg Heigold, Sylvain Gelly, Jakob Uszkoreit, and Neil Houlsby. An image is worth 16x16 words: Transformers for image recognition at scale. In *International Conference on Learning Representations*, 2021.
- [5] Guodong DU, Junlin Lee, Jing Li, Runhua Jiang, Yifei Guo, Shuyang Yu, Hanting Liu, Sim Kuan Goh, Ho-Kin Tang, Daojing He, and Min Zhang. Parameter competition balancing for model merging. In Advances in Neural Information Processing Systems, 2024.
- [6] Ian J Goodfellow, Mehdi Mirza, Da Xiao, Aaron Courville, and Yoshua Bengio. An empirical investigation of catastrophic forgetting in gradient-based neural networks. *arXiv preprint arXiv:1312.6211*, 2013.
- [7] Yifei He, Yuzheng Hu, Yong Lin, Tong Zhang, and Han Zhao. Localize-and-stitch: Efficient model merging via sparse task arithmetic. *Transactions on Machine Learning Research*, 2025.
- [8] Patrick Helber, Benjamin Bischke, Andreas Dengel, and Damian Borth. Eurosat: A novel dataset and deep learning benchmark for land use and land cover classification. *IEEE Journal of Selected Topics in Applied Earth Observations and Remote Sensing*, 12(7):2217–2226, 2019.
- [9] Roger A Horn and Charles R Johnson. Matrix Analysis. Cambridge university press, 2012.
- [10] Edward J Hu, yelong shen, Phillip Wallis, Zeyuan Allen-Zhu, Yuanzhi Li, Shean Wang, Lu Wang, and Weizhu Chen. LoRA: Low-rank adaptation of large language models. In *International Conference on Learning Representations*, 2022.
- [11] Chenyu Huang, Peng Ye, Tao Chen, Tong He, Xiangyu Yue, and Wanli Ouyang. Emr-merging: Tuning-free high-performance model merging. In *Advances in Neural Information Processing Systems*, volume 37, pages 122741–122769, 2024.
- [12] Gabriel Ilharco, Marco Tulio Ribeiro, Mitchell Wortsman, Ludwig Schmidt, Hannaneh Hajishirzi, and Ali Farhadi. Editing models with task arithmetic. In *International Conference on Learning Representations*, 2023.
- [13] Xisen Jin, Xiang Ren, Daniel Preotiuc-Pietro, and Pengxiang Cheng. Dataless knowledge fusion by merging weights of language models. In *International Conference on Learning Representations*, 2023.

- [14] Jonathan Krause, Michael Stark, Jia Deng, and Li Fei-Fei. 3d object representations for fine-grained categorization. In *IEEE International Conference on Computer Vision Workshops*, June 2013.
- [15] Yann LeCun and Corinna Cortes. MNIST handwritten digit database. 2010.
- [16] Yinhan Liu, Myle Ott, Naman Goyal, Jingfei Du, Mandar Joshi, Danqi Chen, Omer Levy, Mike Lewis, Luke Zettlemoyer, and Veselin Stoyanov. Roberta: A robustly optimized bert pretraining approach. arXiv preprint arXiv:1907.11692, 2019.
- [17] Pan Lu, Swaroop Mishra, Tony Xia, Liang Qiu, Kai-Wei Chang, Song-Chun Zhu, Oyvind Tafjord, Peter Clark, and Ashwin Kalyan. Learn to explain: Multimodal reasoning via thought chains for science question answering. In Advances in Neural Information Processing Systems, 2022.
- [18] Zhenyi Lu, Chenghao Fan, Wei Wei, Xiaoye Qu, Dangyang Chen, and Yu Cheng. Twin-merging: Dynamic integration of modular expertise in model merging. In Advances in Neural Information Processing Systems, 2024
- [19] Kenneth Marino, Mohammad Rastegari, Ali Farhadi, and Roozbeh Mottaghi. Ok-vqa: A visual question answering benchmark requiring external knowledge. In *IEEE Conference on Computer Vision and Pattern Recognition*, 2019.
- [20] Michael S Matena and Colin A Raffel. Merging models with fisher-weighted averaging. In *Advances in Neural Information Processing Systems*, volume 35, pages 17703–17716, 2022.
- [21] Niklas Muennighoff, Nouamane Tazi, Loic Magne, and Nils Reimers. MTEB: Massive text embedding benchmark. In *Association for Computational Linguistics*, pages 2014–2037, May.
- [22] Yuval Netzer, Tao Wang, Adam Coates, Alessandro Bissacco, Baolin Wu, Andrew Y Ng, et al. Reading digits in natural images with unsupervised feature learning. In NIPS workshop on deep learning and unsupervised feature learning, volume 2011, page 4, 2011.
- [23] Bryan A. Plummer, Liwei Wang, Chris M. Cervantes, Juan C. Caicedo, Julia Hockenmaier, and Svetlana Lazebnik. Flickr30k entities: Collecting region-to-phrase correspondences for richer image-to-sentence models. In *IEEE International Conference on Computer Vision*, December 2015.
- [24] Alec Radford, Jong Wook Kim, Chris Hallacy, Aditya Ramesh, Gabriel Goh, Sandhini Agarwal, Girish Sastry, Amanda Askell, Pamela Mishkin, Jack Clark, Gretchen Krueger, and Ilya Sutskever. Learning transferable visual models from natural language supervision. In *International Conference on Machine Learning*, volume 139, pages 8748–8763, 18–24 Jul 2021.
- [25] Yujun Shi, Li Yuan, Yunpeng Chen, and Jiashi Feng. Continual learning via bit-level information preserving. In *IEEE Conference on Computer Vision and Pattern Recognition*, pages 16674–16683, June 2021.
- [26] Oleksii Sidorov, Ronghang Hu, Marcus Rohrbach, and Amanpreet Singh. Textcaps: A dataset for image captioning with reading comprehension. In *European Conference on Computer Vision*, pages 742–758, 2020.
- [27] Amanpreet Singh, Vivek Natarajan, Meet Shah, Yu Jiang, Xinlei Chen, Dhruv Batra, Devi Parikh, and Marcus Rohrbach. Towards vqa models that can read. In *IEEE Conference on Computer Vision and Pattern Recognition*, June 2019.
- [28] Johannes Stallkamp, Marc Schlipsing, Jan Salmen, and Christian Igel. The german traffic sign recognition benchmark: A multi-class classification competition. In *International Joint Conference on Neural Networks*, pages 1453–1460, 2011.
- [29] Wenju Sun, Qingyong Li, Yangli-ao Geng, and Boyang Li. Cat merging: A training-free approach for resolving conflicts in model merging. *International Conference on Machine Learning*, 2025.
- [30] Wenju Sun, Qingyong Li, Wen Wang, Yangli ao Geng, and Boyang Li. Task arithmetic in trust region: A training-free model merging approach to navigate knowledge conflicts. arXiv preprint arXiv:2501.15065, 2025.
- [31] Wenju Sun, Qingyong Li, Jing Zhang, Wen Wang, and Yangli-ao Geng. Decoupling learning and remembering: A bilevel memory rramework with knowledge projection for task-incremental learning. In IEEE Conference on Computer Vision and Pattern Recognition, June 2023.
- [32] Anke Tang, Li Shen, Yong Luo, Nan Yin, Lefei Zhang, and Dacheng Tao. Merging multi-task models via weight-ensembling mixture of experts. In *International Conference on Machine Learning*, 2024.

- [33] Alex Wang, Amanpreet Singh, Julian Michael, Felix Hill, Omer Levy, and Samuel R. Bowman. GLUE: A multi-task benchmark and analysis platform for natural language understanding. In *International Conference on Learning Representations*, 2019.
- [34] Ke Wang, Nikolaos Dimitriadis, Guillermo Ortiz-Jimenez, François Fleuret, and Pascal Frossard. Localizing task information for improved model merging and compression. In *International Conference on Machine Learning*, 2024.
- [35] Xun Wu, Shaohan Huang, and Furu Wei. Mixture of loRA experts. In *International Conference on Learning Representations*, 2024.
- [36] Jianxiong Xiao, Krista A Ehinger, James Hays, Antonio Torralba, and Aude Oliva. Sun database: Exploring a large collection of scene categories. *International Journal of Computer Vision*, 119:3–22, 2016.
- [37] Feng Xiong, Runxi Cheng, Wang Chen, Zhanqiu Zhang, Yiwen Guo, Chun Yuan, and Ruifeng Xu. Multi-task model merging via adaptive weight disentanglement. *arXiv preprint arXiv:2411.18729*, 2024.
- [38] Prateek Yadav, Derek Tam, Leshem Choshen, Colin Raffel, and Mohit Bansal. TIES-merging: Resolving interference when merging models. In *Advances in Neural Information Processing Systems*, 2023.
- [39] An Yang, Anfeng Li, Baosong Yang, Beichen Zhang, Binyuan Hui, Bo Zheng, Bowen Yu, Chang Gao, Chengen Huang, Chenxu Lv, et al. Qwen3 technical report. arXiv preprint arXiv:2505.09388, 2025.
- [40] Enneng Yang, Li Shen, Zhenyi Wang, Guibing Guo, Xiaojun Chen, Xingwei Wang, and Dacheng Tao. Representation surgery for multi-task model merging. In *International Conference on Machine Learning*, 2024
- [41] Enneng Yang, Zhenyi Wang, Li Shen, Shiwei Liu, Guibing Guo, Xingwei Wang, and Dacheng Tao. Adamerging: Adaptive model merging for multi-task learning. In *International Conference on Learning Representations*, 2024.
- [42] Jinghan Zhang, shiqi chen, Junteng Liu, and Junxian He. Composing parameter-efficient modules with arithmetic operation. In Advances in Neural Information Processing Systems, volume 36, pages 12589– 12610, 2023.

NeurIPS Paper Checklist

1. Claims

Question: Do the main claims made in the abstract and introduction accurately reflect the paper's contributions and scope?

Answer: [Yes]

Justification: The main claims in the abstract and introduction accurately represent the paper's core contributions, including the motivation behind reducing feature drift, the introduction of LOT Merging, along with detailed board analysis and experimental evaluations.

Guidelines:

- The answer NA means that the abstract and introduction do not include the claims made in the paper.
- The abstract and/or introduction should clearly state the claims made, including the contributions made in the paper and important assumptions and limitations. A No or NA answer to this question will not be perceived well by the reviewers.
- The claims made should match theoretical and experimental results, and reflect how much the results can be expected to generalize to other settings.
- It is fine to include aspirational goals as motivation as long as it is clear that these goals are not attained by the paper.

2. Limitations

Question: Does the paper discuss the limitations of the work performed by the authors?

Answer: [Yes]

Justification: Section 7 discusses the limitations of the proposed method.

Guidelines:

- The answer NA means that the paper has no limitation while the answer No means that the paper has limitations, but those are not discussed in the paper.
- The authors are encouraged to create a separate "Limitations" section in their paper.
- The paper should point out any strong assumptions and how robust the results are to violations of these assumptions (e.g., independence assumptions, noiseless settings, model well-specification, asymptotic approximations only holding locally). The authors should reflect on how these assumptions might be violated in practice and what the implications would be.
- The authors should reflect on the scope of the claims made, e.g., if the approach was only tested on a few datasets or with a few runs. In general, empirical results often depend on implicit assumptions, which should be articulated.
- The authors should reflect on the factors that influence the performance of the approach. For example, a facial recognition algorithm may perform poorly when image resolution is low or images are taken in low lighting. Or a speech-to-text system might not be used reliably to provide closed captions for online lectures because it fails to handle technical jargon.
- The authors should discuss the computational efficiency of the proposed algorithms and how they scale with dataset size.
- If applicable, the authors should discuss possible limitations of their approach to address problems of privacy and fairness.
- While the authors might fear that complete honesty about limitations might be used by reviewers as grounds for rejection, a worse outcome might be that reviewers discover limitations that aren't acknowledged in the paper. The authors should use their best judgment and recognize that individual actions in favor of transparency play an important role in developing norms that preserve the integrity of the community. Reviewers will be specifically instructed to not penalize honesty concerning limitations.

3. Theory assumptions and proofs

Question: For each theoretical result, does the paper provide the full set of assumptions and a complete (and correct) proof?

Answer: [Yes]

Justification: All key formulas in the paper are numbered and accompanied by appropriate derivations or explanations. Formal proofs are provided where necessary, such as the upper bound derivation for feature drift in Section B.

Guidelines:

- The answer NA means that the paper does not include theoretical results.
- All the theorems, formulas, and proofs in the paper should be numbered and crossreferenced.
- All assumptions should be clearly stated or referenced in the statement of any theorems.
- The proofs can either appear in the main paper or the supplemental material, but if they appear in the supplemental material, the authors are encouraged to provide a short proof sketch to provide intuition.
- Inversely, any informal proof provided in the core of the paper should be complemented by formal proofs provided in appendix or supplemental material.
- Theorems and Lemmas that the proof relies upon should be properly referenced.

4. Experimental result reproducibility

Question: Does the paper fully disclose all the information needed to reproduce the main experimental results of the paper to the extent that it affects the main claims and/or conclusions of the paper (regardless of whether the code and data are provided or not)?

Answer: [Yes]

Justification: Section 6.1 and Section C comprehensively describe the experimental configurations, while the code is made available in the supplemental materials.

- The answer NA means that the paper does not include experiments.
- If the paper includes experiments, a No answer to this question will not be perceived well by the reviewers: Making the paper reproducible is important, regardless of whether the code and data are provided or not.
- If the contribution is a dataset and/or model, the authors should describe the steps taken to make their results reproducible or verifiable.
- Depending on the contribution, reproducibility can be accomplished in various ways. For example, if the contribution is a novel architecture, describing the architecture fully might suffice, or if the contribution is a specific model and empirical evaluation, it may be necessary to either make it possible for others to replicate the model with the same dataset, or provide access to the model. In general, releasing code and data is often one good way to accomplish this, but reproducibility can also be provided via detailed instructions for how to replicate the results, access to a hosted model (e.g., in the case of a large language model), releasing of a model checkpoint, or other means that are appropriate to the research performed.
- While NeurIPS does not require releasing code, the conference does require all submissions to provide some reasonable avenue for reproducibility, which may depend on the nature of the contribution. For example
 - (a) If the contribution is primarily a new algorithm, the paper should make it clear how to reproduce that algorithm.
 - (b) If the contribution is primarily a new model architecture, the paper should describe the architecture clearly and fully.
- (c) If the contribution is a new model (e.g., a large language model), then there should either be a way to access this model for reproducing the results or a way to reproduce the model (e.g., with an open-source dataset or instructions for how to construct the dataset).
- (d) We recognize that reproducibility may be tricky in some cases, in which case authors are welcome to describe the particular way they provide for reproducibility. In the case of closed-source models, it may be that access to the model is limited in some way (e.g., to registered users), but it should be possible for other researchers to have some path to reproducing or verifying the results.

5. Open access to data and code

Question: Does the paper provide open access to the data and code, with sufficient instructions to faithfully reproduce the main experimental results, as described in supplemental material?

Answer: [Yes]

Justification: The source code for all experiments is included in the supplemental materials. All datasets used are well-established benchmarks that are publicly accessible.

Guidelines:

- The answer NA means that paper does not include experiments requiring code.
- Please see the NeurIPS code and data submission guidelines (https://nips.cc/public/guides/CodeSubmissionPolicy) for more details.
- While we encourage the release of code and data, we understand that this might not be possible, so "No" is an acceptable answer. Papers cannot be rejected simply for not including code, unless this is central to the contribution (e.g., for a new open-source benchmark).
- The instructions should contain the exact command and environment needed to run to reproduce the results. See the NeurIPS code and data submission guidelines (https://nips.cc/public/guides/CodeSubmissionPolicy) for more details.
- The authors should provide instructions on data access and preparation, including how to access the raw data, preprocessed data, intermediate data, and generated data, etc.
- The authors should provide scripts to reproduce all experimental results for the new proposed method and baselines. If only a subset of experiments are reproducible, they should state which ones are omitted from the script and why.
- At submission time, to preserve anonymity, the authors should release anonymized versions (if applicable).
- Providing as much information as possible in supplemental material (appended to the paper) is recommended, but including URLs to data and code is permitted.

6. Experimental setting/details

Question: Does the paper specify all the training and test details (e.g., data splits, hyperparameters, how they were chosen, type of optimizer, etc.) necessary to understand the results?

Answer: [Yes]

Justification: Section 6.1 and Section C comprehensively describe the experimental configurations.

Guidelines:

- The answer NA means that the paper does not include experiments.
- The experimental setting should be presented in the core of the paper to a level of detail that is necessary to appreciate the results and make sense of them.
- The full details can be provided either with the code, in appendix, or as supplemental material.

7. Experiment statistical significance

Question: Does the paper report error bars suitably and correctly defined or other appropriate information about the statistical significance of the experiments?

Answer: [Yes]

Justification: Section D.5 provide results with random runs.

- The answer NA means that the paper does not include experiments.
- The authors should answer "Yes" if the results are accompanied by error bars, confidence intervals, or statistical significance tests, at least for the experiments that support the main claims of the paper.

- The factors of variability that the error bars are capturing should be clearly stated (for example, train/test split, initialization, random drawing of some parameter, or overall run with given experimental conditions).
- The method for calculating the error bars should be explained (closed form formula, call to a library function, bootstrap, etc.)
- The assumptions made should be given (e.g., Normally distributed errors).
- It should be clear whether the error bar is the standard deviation or the standard error
 of the mean.
- It is OK to report 1-sigma error bars, but one should state it. The authors should preferably report a 2-sigma error bar than state that they have a 96% CI, if the hypothesis of Normality of errors is not verified.
- For asymmetric distributions, the authors should be careful not to show in tables or figures symmetric error bars that would yield results that are out of range (e.g. negative error rates).
- If error bars are reported in tables or plots, The authors should explain in the text how they were calculated and reference the corresponding figures or tables in the text.

8. Experiments compute resources

Question: For each experiment, does the paper provide sufficient information on the computer resources (type of compute workers, memory, time of execution) needed to reproduce the experiments?

Answer: [Yes]

Justification: Section C.1 details the computational resources employed in our experiments, while Section D.6 presents a comprehensive analysis of execution time complexity.

Guidelines:

- The answer NA means that the paper does not include experiments.
- The paper should indicate the type of compute workers CPU or GPU, internal cluster, or cloud provider, including relevant memory and storage.
- The paper should provide the amount of compute required for each of the individual experimental runs as well as estimate the total compute.
- The paper should disclose whether the full research project required more compute than the experiments reported in the paper (e.g., preliminary or failed experiments that didn't make it into the paper).

9. Code of ethics

Question: Does the research conducted in the paper conform, in every respect, with the NeurIPS Code of Ethics https://neurips.cc/public/EthicsGuidelines?

Answer: [Yes]

Justification: The authors have read the NeurIPS Code of Ethics.

Guidelines:

- The answer NA means that the authors have not reviewed the NeurIPS Code of Ethics.
- If the authors answer No, they should explain the special circumstances that require a
 deviation from the Code of Ethics.
- The authors should make sure to preserve anonymity (e.g., if there is a special consideration due to laws or regulations in their jurisdiction).

10. Broader impacts

Question: Does the paper discuss both potential positive societal impacts and negative societal impacts of the work performed?

Answer: [NA]

Justification: This paper advances machine learning methodology through theoretical innovation, with experimental validation conducted on established public datasets. The research focuses on algorithmic improvements rather than direct societal applications.

- The answer NA means that there is no societal impact of the work performed.
- If the authors answer NA or No, they should explain why their work has no societal impact or why the paper does not address societal impact.
- Examples of negative societal impacts include potential malicious or unintended uses (e.g., disinformation, generating fake profiles, surveillance), fairness considerations (e.g., deployment of technologies that could make decisions that unfairly impact specific groups), privacy considerations, and security considerations.
- The conference expects that many papers will be foundational research and not tied to particular applications, let alone deployments. However, if there is a direct path to any negative applications, the authors should point it out. For example, it is legitimate to point out that an improvement in the quality of generative models could be used to generate deepfakes for disinformation. On the other hand, it is not needed to point out that a generic algorithm for optimizing neural networks could enable people to train models that generate Deepfakes faster.
- The authors should consider possible harms that could arise when the technology is being used as intended and functioning correctly, harms that could arise when the technology is being used as intended but gives incorrect results, and harms following from (intentional or unintentional) misuse of the technology.
- If there are negative societal impacts, the authors could also discuss possible mitigation strategies (e.g., gated release of models, providing defenses in addition to attacks, mechanisms for monitoring misuse, mechanisms to monitor how a system learns from feedback over time, improving the efficiency and accessibility of ML).

11. Safeguards

Question: Does the paper describe safeguards that have been put in place for responsible release of data or models that have a high risk for misuse (e.g., pretrained language models, image generators, or scraped datasets)?

Answer: [NA]

Justification: Our work develops machine learning methodologies that are architecture-agnostic and evaluated on conventional datasets. As we do not release pretrained models, scraped datasets, or generative systems, the question of misuse potential does not directly apply to the current contribution.

Guidelines:

- The answer NA means that the paper poses no such risks.
- Released models that have a high risk for misuse or dual-use should be released with
 necessary safeguards to allow for controlled use of the model, for example by requiring
 that users adhere to usage guidelines or restrictions to access the model or implementing
 safety filters.
- Datasets that have been scraped from the Internet could pose safety risks. The authors should describe how they avoided releasing unsafe images.
- We recognize that providing effective safeguards is challenging, and many papers do
 not require this, but we encourage authors to take this into account and make a best
 faith effort.

12. Licenses for existing assets

Question: Are the creators or original owners of assets (e.g., code, data, models), used in the paper, properly credited and are the license and terms of use explicitly mentioned and properly respected?

Answer: [Yes]

Justification: Our paper provides comprehensive citations of related work in the field. The accompanying source code will be released in full compliance with all applicable open-source licenses, with clear attribution given to any incorporated external code.

- The answer NA means that the paper does not use existing assets.
- The authors should cite the original paper that produced the code package or dataset.

- The authors should state which version of the asset is used and, if possible, include a URL.
- The name of the license (e.g., CC-BY 4.0) should be included for each asset.
- For scraped data from a particular source (e.g., website), the copyright and terms of service of that source should be provided.
- If assets are released, the license, copyright information, and terms of use in the
 package should be provided. For popular datasets, paperswithcode.com/datasets
 has curated licenses for some datasets. Their licensing guide can help determine the
 license of a dataset.
- For existing datasets that are re-packaged, both the original license and the license of the derived asset (if it has changed) should be provided.
- If this information is not available online, the authors are encouraged to reach out to the asset's creators.

13. New assets

Question: Are new assets introduced in the paper well documented and is the documentation provided alongside the assets?

Answer: [Yes]

Justification: We will follow these instructions.

Guidelines:

- The answer NA means that the paper does not release new assets.
- Researchers should communicate the details of the dataset/code/model as part of their submissions via structured templates. This includes details about training, license, limitations, etc.
- The paper should discuss whether and how consent was obtained from people whose asset is used.
- At submission time, remember to anonymize your assets (if applicable). You can either create an anonymized URL or include an anonymized zip file.

14. Crowdsourcing and research with human subjects

Question: For crowdsourcing experiments and research with human subjects, does the paper include the full text of instructions given to participants and screenshots, if applicable, as well as details about compensation (if any)?

Answer: [NA]

Justification: The paper does not involve crowdsourcing nor research with human subjects.

Guidelines:

- The answer NA means that the paper does not involve crowdsourcing nor research with human subjects.
- Including this information in the supplemental material is fine, but if the main contribution of the paper involves human subjects, then as much detail as possible should be included in the main paper.
- According to the NeurIPS Code of Ethics, workers involved in data collection, curation, or other labor should be paid at least the minimum wage in the country of the data collector.

15. Institutional review board (IRB) approvals or equivalent for research with human subjects

Question: Does the paper describe potential risks incurred by study participants, whether such risks were disclosed to the subjects, and whether Institutional Review Board (IRB) approvals (or an equivalent approval/review based on the requirements of your country or institution) were obtained?

Answer: [NA]

Justification: The paper does not involve crowdsourcing nor research with human subjects. Guidelines:

- The answer NA means that the paper does not involve crowdsourcing nor research with human subjects.
- Depending on the country in which research is conducted, IRB approval (or equivalent) may be required for any human subjects research. If you obtained IRB approval, you should clearly state this in the paper.
- We recognize that the procedures for this may vary significantly between institutions and locations, and we expect authors to adhere to the NeurIPS Code of Ethics and the guidelines for their institution.
- For initial submissions, do not include any information that would break anonymity (if applicable), such as the institution conducting the review.

16. Declaration of LLM usage

Question: Does the paper describe the usage of LLMs if it is an important, original, or non-standard component of the core methods in this research? Note that if the LLM is used only for writing, editing, or formatting purposes and does not impact the core methodology, scientific rigorousness, or originality of the research, declaration is not required.

Answer: [Yes]

Justification: An LLM was used only for grammar and wording improvements. It played no role in the research methodology or scientific contributions.

- The answer NA means that the core method development in this research does not involve LLMs as any important, original, or non-standard components.
- Please refer to our LLM policy (https://neurips.cc/Conferences/2025/LLM) for what should or should not be described.

A Pseudo Code

Algorithm 1 outlines the proposed LOT merging process. Given a pre-trained model and a set of task vectors, we first extract input features from exemplar sets using task-specific adapters. Then, for each layer, we compute the optimal merged task vector by minimizing the discrepancy between the adapted and reference features. The final model is obtained by linearly combining the pre-trained weights with the optimized task vectors.

Algorithm 1: The model merging process

```
Input: Pre-trained model W_{\mathrm{pre}}; Task vectors \{T_1,\ldots,T_K\}; Exemplar set \{M_1,\ldots,M_K\} Output: Merged model W_{\mathrm{mtl}}^{\mathrm{lot}}

1 T^* = \{T^{1^*},\ldots,T^{L^*}\} // Initial // Collect the input features

2 for k=1 to K do

3 | Initialize task inputs: X_k^1 = M_k

4 | for l=1 to L do

5 | X_k^{l+1} = f(X_k^l;W_0^l + T_k^l)

// Compute optimal task vector for each layer

6 for l=1 to L do

| // Refer to (9), (12) & (14).

7 | T^{l^*} = \arg\min_{T^l} \sum_{k=1}^K \|f_k^l(W_{\mathrm{pre}}^l + T^l) - f_k^l(W_{\mathrm{pre}}^l + T_k^l)\|^2

8 // Merging

9 W_{\mathrm{mtl}}^{\mathrm{lot}} = W_{\mathrm{pre}} + \lambda T^*

10 return W_{\mathrm{mtl}}^{\mathrm{lot}}
```

B Proof of Eq. (5)

Let W_k be the parameters for task k, and let T be a task vector. The feature dirt at layer l caused by T_i is defined as:

$$\Delta f_k^l = f_k^l(W_{pre} + T^l) - f_k^l(W_k).$$

We aim to prove the following bound:

$$|\Delta \mathcal{L}_k| \le \beta \sum_{l=1}^L \left(\prod_{m=l+1}^L \gamma_m \right) \|\Delta f_k^l\|, \tag{21}$$

where \mathcal{L} is assumed β -Lipschitz continuous with respect to the network's final output, and each layer l is γ_l -Lipschitz continuous with respect to its input (i.e., the output of layer l-1) within the merging region.

Proof. The feature shift at layer l can be decomposed as:

$$f_k^l(W_{pre} + T) - f_k^l(W_k) = f_k^l(f_k^{l-1}(W_{pre} + T); W_{pre} + T^l) - f_k^l(f_k^{l-1}(W_k); W_k)$$

$$= f_k^l(f_k^{l-1}(W_{pre} + T); W_{pre} + T^l) - f_k^l(f_k^{l-1}(W_k); W_{pre} + T^l)$$

$$+ f_k^l(f_k^{l-1}(W_k); W_{pre} + T^l) - f_k^l(f_k^{l-1}(W_k); W_k).$$
(22)

Under the norm-induced triangular inequality, we have:

$$||f_{k}^{l}(W_{pre} + T) - f_{k}^{l}(W_{k})|| \le ||f_{k}^{l}(f_{k}^{l-1}(W_{pre} + T); W_{pre} + T^{l}) - f_{k}^{l}(f_{k}^{l-1}(W_{k}); W_{pre} + T^{l})|| + ||f_{k}^{l}(f_{k}^{l-1}(W_{k}); W_{pre} + T^{l}) - f_{k}^{l}(f_{k}^{l-1}(W_{k}); W_{k})||.$$

$$(23)$$

- For the first part, we apply the γ_l -Lipschitz continuity of f_k^l :

$$\|f_k^l(f_k^{l-1}(W_{pre}+T);W_{pre}+T^l)-f_k^l(f_k^{l-1}(W_k);W_{pre}+T^l)\|\leq \gamma_l\|f_k^{l-1}(W_{pre}+T)-f_k^{l-1}(W_k)\|.$$

- For the second part:

$$\|f_k^l(f_k^{l-1}(W_k);W_{pre}+T^l)-f_k^l(f_k^{l-1}(W_k);W_k)\|=\|\Delta f_k^l\|.$$

Combining these two terms, we have:

$$||f_k^l(W_{pre} + T) - f_k^l(W_k)|| \le \gamma_l ||f_k^{l-1}(W_{pre} + T) - f_k^{l-1}(W_k)|| + ||\Delta f_k^l||.$$

Unfolding this recursive inequality from l = 1 to l = L and accumulating the error gives:

$$||f_k^L(W_{pre} + T) - f_k^L(W_k)|| \le \sum_{l=1}^L \left(\prod_{m=l+1}^L \gamma_m\right) ||\Delta f_k^l||.$$
 (24)

Using the assumption that \mathcal{L} is β -Lipschitz continuous with respect to the network's final output, we conclude:

$$|\Delta \mathcal{L}_k| \le \beta \sum_{l=1}^L \left(\prod_{m=l+1}^L \gamma_m \right) \|\Delta f_k^l\|. \tag{25}$$

C Experimental Setup

This section provides an overview of the experimental setup, including details about the computational environment, datasets, and the baseline models employed in the experiments.

C.1 Computational Resources

All experiments described in this paper were performed on a workstation running Ubuntu 16.04. The system configuration includes dual Intel Xeon 2.60GHz CPUs, 256 GB of RAM, and six NVIDIA RTX 3090 GPUs. The code was implemented in Python 3.8 and executed on this hardware platform to ensure consistency across all experiments.

C.2 Datasets

Our experimental procedure follows the guidelines outlined in Task Arithmetic [12], utilizing eight commonly used image classification datasets, which are summarized below:

- SUN397 [36]: A large-scale dataset comprising 108,754 images, organized into 397 categories. Each category contains a minimum of 100 images, making this dataset a comprehensive benchmark for scene classification tasks.
- **Stanford Cars** [14]: A fine-grained dataset with 16,185 images of 196 distinct car models. The dataset is split evenly into training and testing sets, providing a reliable resource for evaluating car model recognition systems.
- **RESISC45** [2]: This remote sensing dataset consists of 31,500 images representing 45 different scene categories. Each category contains around 700 images, covering a broad range of geographical and structural themes.
- EuroSAT [8]: A satellite image dataset containing 27,000 labeled and geo-referenced images. The dataset is divided into 10 categories, including forests, urban areas, and agricultural fields, designed for land-use classification tasks.
- **SVHN** [22]: This dataset, derived from real-world street view images, consists of 73,257 training and 26,032 test images of digits, distributed across 10 classes. An additional 531,131 samples are included for extended training purposes.

- **GTSRB** [28]: The German Traffic Sign Recognition Benchmark, which includes over 50,000 images across 43 traffic sign categories. This dataset is a well-known benchmark for traffic sign recognition systems.
- MNIST [15]: A foundational dataset for handwritten digit classification, consisting of 60,000 training images and 10,000 test images, distributed across 10 digit classes.
- **DTD** [3]: A dataset designed for texture classification, containing 5,640 images across 47 categories, with approximately 120 images per category. It is commonly used for evaluating texture recognition algorithms.

In addition, we also utilize six vision-language datasets, which are detailed below:

- **COCO Caption** [1]: A large image captioning dataset derived from the MS COCO collection. It contains over 330,000 images, each annotated with five different captions, aimed at training models to generate natural language descriptions for images.
- Flickr30k Caption [23]: This dataset consists of 31,000 images from Flickr, with each image paired with five descriptive sentences. It is used for both image captioning and retrieval tasks.
- **TextCaps** [26]: A challenging dataset for image captioning, where the captions require reasoning over both visual and textual information present within the image. The dataset includes 145,000 image-caption pairs.
- **OKVQA** [19]: A knowledge-based visual question answering dataset that includes over 14,000 questions requiring external knowledge to answer. The dataset is designed to assess reasoning beyond visual content alone.
- **TextVQA** [27]: A visual question answering dataset that emphasizes reading and interpreting text embedded within images. It contains over 45,000 questions across 28,000 images, necessitating both visual and textual reasoning.
- **ScienceQA** [17]: A multi-modal dataset for scientific question answering, consisting of over 21,000 multiple-choice questions paired with images and textual explanations across various scientific disciplines, including biology, chemistry, and physics.

C.3 Baseline Methods

In this study, we compare our approach with several baseline methods. Below, we provide a description of each baseline:

- **Pre-trained**: This baseline uses a pre-trained model to perform tasks across multiple domains. Since it does not leverage any task-specific fine-tuning, it typically results in suboptimal performance on downstream tasks.
- **Individual**: In this method, separate models are fine-tuned for each task individually. Although this avoids task interference, it is limited by the inability to perform multi-task learning simultaneously. It represents a reference for the best possible performance, or *upper bound*, for merging methods.
- **Traditional MTL**: This approach combines the training data from all tasks and trains a single multi-task model. It serves as a traditional method for joint task learning.

The following are compression-based approaches:

- **EMR Merging** [11]: This method applies lightweight task-specific masks and rescalers to compress task vectors.
- **WEMOE** [32]: Upscales MLP layers into input-dependent Mixture-of-Experts modules to dynamically integrate shared and task-specific knowledge during model merging.

The following are test-time training-based approaches:

• AdaMerging [41]: This method adapts the model to new tasks by using an unlabeled test set to learn adaptive merging coefficients at both the task- and layer-level, as applied in Task Arithmetic.

- AdaMerging++ [41]: An improved version of AdaMerging, which integrates the principles of Ties-Merging [38] to further enhance the adaptive merging process.
- Surgery [40]: Surgery introduces a feature transformation module that aligns the features from different tasks during the merging process. In our experiments, we utilize the basic version of Surgery alongside Task Arithmetic for evaluation.
- Localize-and-Stitch [7]: This method optimally combines the strengths of several fine-tuned models by identifying and localizing essential regions within each model before merging.

The following methods do not require training:

- Weight Averaging: This technique averages the parameters from the models of different tasks to form a single multi-task model without any additional training steps.
- **Fisher Merging** [20]: This approach uses the Fisher information matrix to assess the relative importance of model parameters, merging them based on their significance.
- **RegMean** [13]: RegMean adjusts and combines rows from weight matrices based on statistical information gathered from the training data, refining the model's parameters.
- Task Arithmetic [12]: Task Arithmetic introduces the concept of a "task vector," which is defined as the difference between fine-tuned model parameters and pre-trained model parameters. By combining multiple task vectors and adding them to the pre-trained model, it enables multi-task learning.
- **Ties-Merging** [38]: Ties-Merging removes insignificant parameters from the task vectors and resolves sign conflicts, reducing interference during the merging of task vectors.
- TATR [30]: TATR improves upon Task Arithmetic by restricting the merging of task vectors to a defined trust region, which reduces knowledge conflicts between tasks.
- TATR & Ties-Merging [30, 38]: This method combines the trust region restriction of TATR with Ties-Merging to further enhance task vector merging.
- **Consensus Merging** [34]: This method computes a set of masks for each task vector to minimize the distance between the merged model and each fine-tuned model in the parameter space.
- AWD Merging [37]: AWD Merging generates redundant vectors such that subtracting them from the original task vectors leads to increased orthogonality in the remaining vectors.
- **PCB Merging** [5]: PCB Merging trims components of the task vector that have small magnitudes and are not strongly correlated with other tasks.
- **CAT Merging** [29]: CAT Merging trims components (using projection or mask) of the task vector that may cause knowledge conflicts.

D Additional Experiments

D.1 Additional Performance Comparision

In this section, we compare LOT Merging with both compression-based methods and test-time adaptation-based approaches. Compression-based methods rely on techniques such as masking [11] or singular value decomposition (SVD) [32] to compress task vectors, and typically require manually specified or trained routers during inference to select the appropriate task vector. On the other hand, test-time adaptation-based methods leverage unlabeled test data to train merging weights or certain modules, which introduces additional computational overhead and data requirements.

It is important to note that comparing LOT Merging with these methods is inherently **unfair**, as LOT Merging is a training-free approach and does not require any adaptation or auxiliary modules at inference time. Moreover, the merged model of LOT Merging retains the original network architecture without introducing any structural modifications. As shown in Table 4, while LOT Merging lags behind compression-based methods in terms of average accuracy, it achieves comparable or even superior performance to several representative test-time adaptation approaches. This highlights the strength of LOT Merging in competitive performance across diverse vision tasks.

Table 4: Multi-task performance when merging on eight vision tasks. Results of Localize-and-Stitch with "†" stem from the original paper, where only the performance on ViT-B/32 is provided.

Method	SUN397	Cars	RESISC45	EuroSAT	SVHN	GTSRB	MNIST	DTD	Avg Acc			
			,	ViT-B/32								
			Compress	ion based me	thods							
WEMOE	74.1	77.4	93.7	99.1	96.2	98.9	99.6	76.4	89.4			
EMR-Merging	75.2	72.8	93.5	99.5	96.9	98.1	99.6	74.4	88.7			
Test-time Adaption based methods												
TW AdaMerging	58.0	53.2	68.8	85.7	81.1	84.4	92.4	44.8	71.1			
TW AdaMerging++	60.8	56.9	73.1	83.4	87.3	82.4	95.7	50.1	73.7			
LW AdaMerging	64.5	68.1	79.2	93.8	87.0	91.9	97.5	59.1	80.1			
LW AdaMerging++	66.6	68.3	82.2	94.2	89.6	89.0	98.3	60.6	81.1			
Surgery Merging	63.8	59.9	83.3	97.9	87.0	87.0	98.6	69.4	80.9			
Localize-and-Stitch [†]	67.2	68.3	81.8	89.4	87.9	86.6	94.8	62.9	79.9			
Training-free methods												
LOT Merging (ours)	67.7	67.5	85.7	94.9	93.4	89.8	98.7	63.6	82.7			
				ViT-L/14								
			Compress	ion based me	thods							
WEMOE	81.4	92.6	95.4	99.4	97.7	99.3	99.7	83.7	93.6			
EMR-Merging	83.2	90.7	96.8	99.7	97.9	99.1	99.7	82.7	93.7			
			Test-time Add	aption based	methods							
AdaMerging	79.0	90.3	90.8	96.2	93.4	98.0	99.0	79.9	90.8			
AdaMerging++	79.4	90.3	91.6	97.4	93.4	97.5	99.0	79.2	91.0			
Surgery Merging	75.7	84.4	93.1	98.8	91.3	93.4	99.1	76.1	89.0			
			Trainir	ig-free metho	ds							
LOT Merging (ours)	76.7	88.6	91.7	98.7	97.1	95.7	99.5	76.4	90.5			

Table 5: Multi-task performance when merging ViT-B/16 models on eight tasks.

Method	SUN397	Cars	RESISC45	EuroSAT	SVHN	GTSRB	MNIST	DTD	Avg Acc
Pre-trained	63.8	64.6	65.7	54.5	52.0	43.3	51.7	45.1	55.0
Individual	81.8	86.8	96.9	99.7	97.8	99.1	99.7	82.0	92.9
Weight Averaging	67.7	70.0	75.3	79.5	74.9	60.1	94.4	43.8	70.7
Fisher Merging	68.5	69.9	75.2	80.4	73.2	61.2	94.5	50.7	71.7
RegMean	69.1	71.6	77.6	88.8	83.7	70.2	96.9	54.6	76.6
Task Arithmetic	61.1	65.9	74.0	76.2	88.0	73.9	98.4	53.0	73.8
Ties-Merging	69.1	72.5	80.5	84.0	85.0	71.5	98.1	54.9	77.0
TATR	67.4	70.4	77.9	81.7	87.6	77.2	98.3	55.6	77.0
AWD Merging	67.8	72.7	78.7	88.5	90.9	83.6	98.9	57.1	79.8
CAT Merging	72.9	75.9	83.1	92.8	88.2	82.7	98.8	62.7	82.1
LOT Merging (ours)	71.0	76.2	87.6	95.8	96.5	91.9	99.2	67.0	85.7

D.2 Comparison on ViT-B/16

Table 5 presents the multi-task performance of various model merging techniques on eight diverse tasks using ViT-B/16. As can be seen, LOT Merging outperforms all baselines, achieving the highest average accuracy (85.7%). Notably, it excels in almost all tasks, demonstrating its ability to balance task-specific feature retention and shared information utilization. These results highlight the effectiveness of LOT Merging in multi-task learning scenarios.

D.3 Analysis of Exemplar Number

Table 6 presents the multi-task performance of LOT Merging with varying numbers of exemplars. The results are shown for both the ViT-B/32 and ViT-L/14 models with different numbers of exemplars used for merging, ranging from 4 to 64. As the number of exemplars increases, we observe a consistent improvement in performance across all datasets for both ViT architectures. Notably, LOT Merging already achieves state-of-the-art performance with only 8 exemplars per task, demonstrating that LOT Merging is particularly well-suited for dataless adaptation settings.

Table 6: Multi-task performance of LOT Merging with various numbers of exemplars. The "#exemplar" column represents the number of exemplars used for merging.

#exemplar	SUN397	Cars	RESISC45	EuroSAT	SVHN	GTSRB	MNIST	DTD	Avg Acc
				ViT-B/32	!				
4	64.2	64.3	69.1	84.4	88.6	77.9	96.5	51.1	74.5
8	65.4	66.3	79.4	87.6	92.8	85.5	98.2	54.1	78.7
16	66.4	67.1	82.6	90.9	91.7	86.1	98.5	58.1	80.2
32	67.4	67.5	83.3	92.4	93.2	89.6	98.6	60.6	81.6
64	67.7	67.5	85.7	94.9	93.4	89.8	98.7	63.6	82.7
				ViT-L/14	!				
4	74.1	87.5	86.6	92.6	95.3	92.1	99.1	66.5	86.7
8	75.4	87.8	88.4	95.9	96.4	93.9	99.3	68.3	88.2
16	75.7	87.6	89.0	98.2	96.6	94.0	99.4	71.3	89.0
32	76.4	88.4	91.2	98.3	97.0	95.5	99.5	74.1	90.0
64	76.7	88.6	91.7	98.7	97.1	95.7	99.5	76.4	90.5

Table 7: Ablation Study of LOT Merging.

Linear Weight	Scaler	Bias S	UN397	Cars	RESISC45	EuroSAT	SVHN	GTSRB	MNIST	DTD	Avg Acc
				Vi	T-B/32						
	✓	✓	61.9	57.4	60.4	55.9	36.2	30.0	54.3	42.3	49.8
✓		✓	67.8	67.9	85.9	92.6	93.3	87.5	98.7	62.0	81.9
✓	\checkmark		67.9	67.7	84.6	93.5	93.2	90.5	98.2	64.0	82.4
\checkmark	\checkmark	✓	67.7	67.5	85.7	94.9	93.4	89.8	98.7	63.6	82.7
				Vi	T-L/14						
	\checkmark	✓	67.3	78.5	72.3	64.6	59.5	50.4	76.7	55.6	65.6
✓		✓	76.7	88.4	92.4	98.4	97.0	94.8	99.5	75.3	90.3
✓	✓		76.3	88.3	91.7	98.6	97.1	95.2	99.5	75.3	90.2
✓	\checkmark	✓	76.7	88.6	91.7	98.7	97.1	95.7	99.5	76.4	90.5

D.4 Ablation Study

In this ablation study, we investigate the impact of merging pre-trained and learned parameters on the performance of Vision Transformers (ViT). Specifically, we examine three types of parameters: linear weight, scaling factors, and bias coefficient. For each type, we replace the merged parameters with the pre-trained ones and evaluate the effect on model performance.

The results, shown in Table 7, demonstrate that merging each type of parameter leads to consistent improvements across the board. Among the three parameter types, merging the Linear Weight yields the largest performance boost, as it represents the majority of the model's parameters.

Table 8: Multi-task performance of LOT Merging with three random exemplar sets.

	SUN397	Cars	RESISC45	EuroSAT	SVHN	GTSRB	MNIST	DTD Avg A	cc	
VIT-B/32										
Random exemplar set 1	67.8	67.5	85.3	94.6	93.4	89.8	98.7	63.9 82.6		
Random exemplar set 2	67.6	67.5	85.8	94.6	93.7	89.2	98.6	63.9 82.6		
Random exemplar set 3	67.7	67.7	86.1	95.6	93.3	90.5	98.7	63.1 82.8		
Average	67.7	67.5	85.7	94.9	93.4	89.8	98.7	63.6 82.7		
			Vi	T-L/14						
Random exemplar set 1	76.7	88.8	91.5	98.7	97.0	95.7	99.6	76.3 90.5		
Random exemplar set 2	76.8	88.3	91.6	98.8	97.1	95.5	99.5	76.5 90.5		
Random exemplar set 3	76.6	88.6	91.9	98.4	97.0	95.9	99.4	76.3 90.5		
Average	76.7	88.6	91.7	98.7	97.1	95.7	99.5	76.4 90.5		

D.5 Robustness Analysis of Exemplar Sets

Table 8 demonstrates the robustness of LOT Merging across three random exemplar sets. For both ViT-B/32 and ViT-L/14, the average accuracy remains highly stable ($\leq 0.2\%$ variance), with minimal fluctuations across datasets. The stronger ViT-L/14 backbone further enhances stability, maintaining a consistent 90.5% average accuracy. These results confirm that LOT Merging is highly robust to exemplar selection, ensuring reliable performance across diverse tasks.

Table 9: Computational complexity comparison (in seconds) for merging ViT-B/32 and ViT-L/14 models across eight vision tasks, measured on a single RTX 3090 GPU.

Method TA w/ Surgery	AdaMerging	TATR	PCB Merging	CAT Merging	LOT Merging (ours)
ViT-B/32 12621	8276	176	43	46	44
ViT-L/14 36826	16299	283	131	150	161

D.6 Analysis of Computational Complexity

The computational overhead of LOT Merging is reasonable and practically efficient. The procedure consists of two primary stages:

- **Feature extraction:** This step is highly efficient, requiring only a small number of unlabeled examples (typically 16–64 per task). As it avoids training or gradient-based updates, the computational cost remains minimal;
- Optimal task-vector computation: This step relies on a closed-form solution, eliminating the need for iterative optimization. For linear task representations, this involves a matrix inversion operation. While matrix inversion can be associated with higher theoretical complexity $(\mathcal{O}(d^3))$, we mitigate this overhead through parallelized implementation on modern GPUs. In practice, the computation is highly efficient and introduces negligible latency.

Empirical runtime measurements, summarized in Table 9 (recorded on a single NVIDIA RTX 3090 GPU), confirm that LOT Merging achieves significantly lower wall-clock time compared to training-based baselines such as TA with Surgery [40] and AdaMerging [41]. These results highlight the practical efficiency of our approach, making it highly suitable for scenarios where rapid adaptation across tasks is required.

Table 10: Consistency comparison for merging ViT-B/32 and ViT-L/14 models across eight vision tasks.

	Fisher Merging	RegMean	Task Arithmetic	PCB Merging	CAT Merging	LOT Merging(ours)
ViT-B/32	13.78	8.46	8.95	6.85	6.21	4.58
ViT-L/14	6.79	6.86	5.11	3.49	2.51	2.64

D.7 Analysis of Consistency

While LOT Merging achieves the highest average performance in Tables 1 and 2, it does not consistently deliver the best accuracy on every individual dataset. This variation can be attributed to methods like Fisher merging, which tend to yield uneven performance across tasks. To quantify such inconsistency, we compute the standard deviation of accuracy drops—defined as the difference between the task-specific and merged model accuracies—across all tasks. As shown in Table 10, LOT Merging exhibits low variance, indicating a more balanced integration of task knowledge without favoring specific tasks.

Table 11: Results (%) on seen and unseen Tasks

	SUN397	Cars	RESISC45	DTD	SVHN	GTSRB	Avg Acc (Seen)	MNIST (Unseen)	EuroSAT (Unseen)	Avg Acc (Unseen)
Task Arithmetic	63.3	62.4	75.1	57.8	84.6	80.4	70.6	77.2	46.2	61.7
Ties-Merging	67.8	66.2	77.2	56.7	77.1	70.9	69.3	75.9	43.3	59.6
LOT Merging	69.1	69.1	89.7	65.6	94.1	93.7	80.2	81.5	45.4	63.5
	SUN397	Cars	GTSRB	EuroSAT	DTD	MNIST	Avg Acc (Seen)	RESISC45 (Unseen)	SVHN (Unseen)	Avg Acc (Unseen)
Task Arithmetic	64.0	64.0	75.2	87.7	57.0	95.7	73.9	52.3	44.9	51.1
Ties-Merging	68.0	67.1	67.7	78.4	56.5	92.8	71.8	58.7	49.2	53.9
LOT Merging	68.8	69.9	84.8	95.8	61.5	97.5	79.7	56.3	54.6	55.5

D.8 Analysis of Generalization Ability

We first evaluated our method by merging models trained on six out of eight tasks and then testing on the remaining two unseen tasks. As shown in the tables 11, LOT Merging consistently outperforms both Task Arithmetic and Ties-Merging—not only on seen tasks, but also on unseen (out-of-domain) tasks. These results demonstrate the moderate generalization ability of our approach. However, the performance gap does become narrower on out-of-domain tasks compared to in-domain tasks.

Table 12: Average accuracy with Gaussian blur kernel

Method	Gaussian Blur Kernel	ViT-B/32 (%)	ViT-L/14 (%)
Task Arithmetic	_	69.1	84.5
LOT Merging	$kernel_size = 3, \sigma = 1$	82.2	90.3
LOT Merging	$kernel_size = 5, \sigma = 2$	80.0	89.5
LOT Merging	$kernel_size = 7, \sigma = 3$	78.3	88.7

Table 13: Performance when using similar distributed exemplars

Method	COCO Caption	OKVQA	ScienceQA
Task Arithmetic	0.53	40.37	51.55
LOT Merging	0.87	44.25	60.08
LOT Merging w/ surrogate exemplars	0.62	40.15	53.54

This observation motivates us to further explore ways to enhance LOT Merging's effectiveness on out-of-domain tasks in future work.

Next, we explored the use of domain-similar auxiliary data by applying a Gaussian blur to the original task exemplars. As shown in Table 12, LOT Merging consistently outperformed Task Arithmetic across all blur levels, although performance gradually declined as blur strength increased.

To investigate whether similar distribution exemplars would benefit, we merged BLIP models fine-tuned on COCO Caption, OKVQA, and ScienceQA, but replaced each task's exemplars with samples from semantically related datasets: Flickr30k for COCO Caption, AOKVQA for OKVQA, and IconQA for ScienceQA. As shown in Table 13, LOT Merging with surrogate exemplars outperforms Task Arithmetic, though the improvements are task-dependent—substantial for COCO Caption, but more limited for the other two.

D.9 Robustness Analysis with Data Corruption

To assess the robustness of LOT Merging under noisy conditions, we adopted the corruption protocol introduced in [41], applying seven types of corruption to both exemplars and test sets. We evaluated the performance by merging eight ViT-B/32 models on each corrupted dataset and compared LOT Merging to Task Arithmetic. Table 14 shows that LOT Merging maintains consistent improvement over Task Arithmetic under all corruption types.

Table 14: Average accuracy under different corruption types

Corruption Type	Task Arithmetic	LOT Merging ($\uparrow \Delta$)
Clean (no corruption)	69.1	82.7 († 13.6)
Motion Blur	47.3	59.9 († 12.6)
Impulse Noise	51.1	60.8 († 9.7)
Gaussian Noise	50.6	60.1 († 9.5)
Pixelate	48.9	61.8 († 12.9)
Spatter	65.0	79.2 († 14.2)
Contrast	38.5	45.9 († 7.4)
JPEG Compression	25.9	28.1 († 2.2)

D.10 Results on Merging Language Models

We conducted experiments using RoBERTa [16] as the backbone on the GLUE benchmark [33], which comprises eight diverse NLP tasks spanning both classification and regression (e.g., stsb). For evaluation, we report accuracy for classification tasks and the average of Pearson and Spearman correlations for the regression task. The results are presented in Table 15. LOT Merging achieves the highest average performance compared to the baseline methods, demonstrating its effectiveness for language model merging.

Table 15: Performance of Different Algorithms on GLUE Tasks

Algorithm	CoLA	MNLI	MRPC	QNLI	QQP	RTE	SST-2	STS-B	Average	#best
Task Arithmetic	6.68	66.23	78.46	78.62	72.69	53.43	83.49	27.10	58.34	1
Ties-Merging	9.46	59.34	74.71	65.93	41.29	47.29	72.13	9.21	47.42	0
PCB Merging	11.40	50.85	77.63	78.22	55.78	60.29	75.57	67.01	59.59	1
CAT Merging	33.20	72.33	68.22	82.92	76.05	62.82	89.33	15.57	62.56	2
LOT Merging	17.13	73.04	78.27	77.22	78.81	65.35	89.74	25.50	63.13	4

Table 16: Performance Comparison when merging two Qwen models.

Method	ArguAna	ArXiv Hierarchical Clustering S2S
Individual	53.62	0.6377
Task Arithmetic	30.86	0.6318
LOT Merging	47.36	0.6374

We also conduct experiments on large language models. We select Qwen3-0.6B [39] as the pretrained backbone, and two official fine-tuned variants—Qwen3-Embedding-0.6B and Qwen3-Reranker-0.6B. Although Qwen3-0.6B has a relatively small parameter count, it features a deep architecture with 28 Qwen3DecoderBlocks, each comprising an attention module (four projection linear layers) and an MLP module (three projection linear layers), for a total of 196 linear layers.

To reflect their respective strengths in embedding and ranking, we selected two tasks from the MTEB (English, v2) benchmark [21]: ArguAna — a retrieval task requiring strong ranking capabilities; ArXiv Hierarchical Clustering S2S — a clustering task requiring high-quality embeddings. Evaluation metrics were top-1 accuracy for ArguAna and V-measure for ArXiv Hierarchical Clustering. Results in Table 16 demonstrate that LOT Merging substantially outperforms Task Arithmetic on ArguAna, indicating improved cross-task transfer for ranking, while maintaining competitive clustering performance. These results confirm that our method remains effective on deep LLMs such as Qwen3. Table 17: Pearson Correlation across Different Tasks

	COCO Caption	Flickr30k Caption	TextCaps	OKVQA	TextVQA	ScienceQA
Pearson Correlation	0.51	0.60	0.30	0.82	0.77	0.20

D.11 Analysis of Feature Drift on Multi-Model Tasks

To assess the impact of feature drift in vision-language settings, we measured the Pearson correlation between feature drift and loss change in BLIP models across several multimodal benchmarks after Task Arithmetic merging. The results in 17 demonstrate that feature drift remains a positively correlated factor.

While the correlation strength varies—reflecting inherent complexities such as reasoning demands and modality interactions—our experiments consistently show that reducing feature drift leads to performance gains, even in vision-language tasks. This suggests that, despite the greater complexity in multimodal models, minimizing feature drift remains an effective and broadly applicable merging objective.

D.12 Robustness Analysis under Real-Time Data Distribution

We further study the impact of real-time data on model performance, particularly in scenarios where exemplars are available for only a subset of classes, while evaluation is conducted on the complete test set. The results in Table 18 show that although LOT Merging's performance declines with fewer exemplar classes, it still consistently outperforms Task Arithmetic.

Table 18: Effect of Exemplar Classes on Average Accuracy

Backbone	Method	Exemplar Classes	Avg. Acc.
ViT-B/32	Task Arithmetic	_	69.1
ViT-B/32	LOT Merging	All classes	82.7
ViT-B/32	LOT Merging	First 1/2	81.8
ViT-B/32	LOT Merging	First 1/3	81.0
ViT-B/32	LOT Merging	First 1/4	79.6
ViT-B/32	LOT Merging	First 1/5	77.6
ViT-L/14	Task Arithmetic	_	84.5
ViT-L/14	LOT Merging	All classes	90.5
ViT-L/14	LOT Merging	First 1/2	90.0
ViT-L/14	LOT Merging	First 1/3	89.6
ViT-L/14	LOT Merging	First 1/4	88.9
ViT-L/14	LOT Merging	First 1/5	88.3